Decorated, Tapered, and Highly Nonlinear Granular Chain

Robert Doney*
U.S. Army Research Laboratory, Aberdeen Proving Grounds, Maryland 21005, USA, and Physics Department, State University of New York, Buffalo, New York 14260-1500, USA

Surajit Sen†
Physics Department, State University of New York, Buffalo, New York 14260-1500, USA

(Received 13 July 2006; published 11 October 2006)

It has been seen that inertial mismatches in 1D granular chains lead to remarkable energy absorption which increases with the number of spheres, N, and tapering, q. Short chains, however, are limited in that regard, and we therefore present one solution which greatly improves performance for any size chain. These strongly nonlinear and scalable systems feature surprisingly complicated dynamics and are inadequately represented by a hard-sphere approximation. Additionally, such systems have shock absorption capacities that vary as a function of position along the chain. In this Letter, we present results in the form of normalized kinetic energy diagrams to illustrate the impressive mitigation capability of both original and improved tapered chains.

DOI: 10.1103/PhysRevLett.97.155502 PACS numbers: 62.50.+p, 05.45.−a, 83.80.Fg

We have reported on a seemingly simple, shock absorbing, 1D dynamical system [1] consisting of an alignment of elastic spheres of progressively smaller radii. We call this system a simple (tapered) chain. This system defeats shocks by spreading impulses out in time and space through inertial mismatches between nearest neighbors [2,3]. The effect has been recently validated experimentally by Nakagawa *et al.* [4] and Melo and collaborators [5]. However, these systems have limited energy dispersion capability for small chains. Herein we report overcoming this challenge by introducing smaller beads of constant radius at each contact point. For convenience, that radius is just some fractional size, f, of the smallest bead's radius, r_N. These systems, now referred to as decorated (tapered) chains, represent a tremendous improvement and are strongly nonlinear. Consequently, a hard-sphere approximation is invalid even though it sufficiently describes a simple chain. In addition, there is promising empirical evidence to support our assertion regarding decorated chains. This report briefly reviews key results of the simple chain followed by the superior ability of the decorated chain—both hard-sphere approximations and numerical work will be presented.

Tapered chain systems represent an alternative to current methods of dealing with undesirable transients, such as ballistic shock, where metal foams and honeycombs are being used [6,7]. When honeycombs are extruded, one obtains a linear cellular alloy [8], which has demonstrated improved energy absorption capabilities [9]. Another approach to dismiss transients is through the use of functionally graded materials [10] where one can introduce impedance mismatches gradually or discontinuously. What tapered chains offer as an improvement to currently available technologies is an inherent scalability, the potential for improved performance, and reduced cost—after all, bearings are inexpensive.

Simple chains are parametrized by the number of spheres, N, and amount of tapering, q_s. We can quantify their efficiency by measuring the normalized kinetic energy, $K_N \equiv K_{\mathrm{OUT}}/K_{\mathrm{IN}}$, where K_{IN} is the initial impulse energy delivered by the first sphere and K_{OUT} is the kinetic energy felt by the last sphere due to the first wave front (reflections are neglected). A hard-sphere study of the elastic collision between particles using energy and linear momentum laws [2] indicate

$$K_N = \left(\frac{4(1-q_s)^3}{[1+(1-q_s)^3]^2}\right)^{N-1}, \tag{1}$$

where the ratio of adjacent radii is defined as $R_{i+1}/R_i = (1-q_s)$ [see Figs. 1(b) and 1(c)]. We have added a subscript to q for reasons that will become clear below.

The spheres can be assumed to interact through the strongly nonlinear Hertz potential [11,12], $V(\delta_{i,i+1}) = \frac{2}{5D}\sqrt{R_i R_{i+1}/(R_i+R_{i+1})}\,\delta_{i,i+1}^{5/2} \equiv a_{i,i+1}\delta_{i,i+1}^{5/2}$, where $\delta_{i,i+1} = R_i + R_{i+1} - (z_{i+1} - z_i)$ represents the overlap of successive grains and z_j is the absolute position of a grain. In addition, the constant, $D = \frac{3}{2}(\frac{1-\sigma^2}{E})$, incorporates material properties [13] of Ti_6Al_4V: the Young's modulus, $E = 114$ kN/mm^2, and Poisson ratio, $\sigma = 0.33$. In addition, for each chain, an initial velocity of 0.01 mm/μs (10 m/s) is applied to the largest end. It is known that, among other constraints, the Hertz potential is valid when impulse speeds are sufficiently less than the sound speed of the material. However, we have begun hydrocode simulations exploring impact velocities up to 1 km/s, which suggest continued energy absorption well beyond 10 m/s [14].

The equations of motion are then given as

$$m_i \ddot{z}_i = \frac{5}{2}\{a_{i-1,i}\delta_{i-1,i}^{3/2} - a_{i,i+1}\delta_{i,i+1}^{3/2}\}. \tag{2}$$

We will focus on the evaluation of K_N [Fig. 1(a)]. The

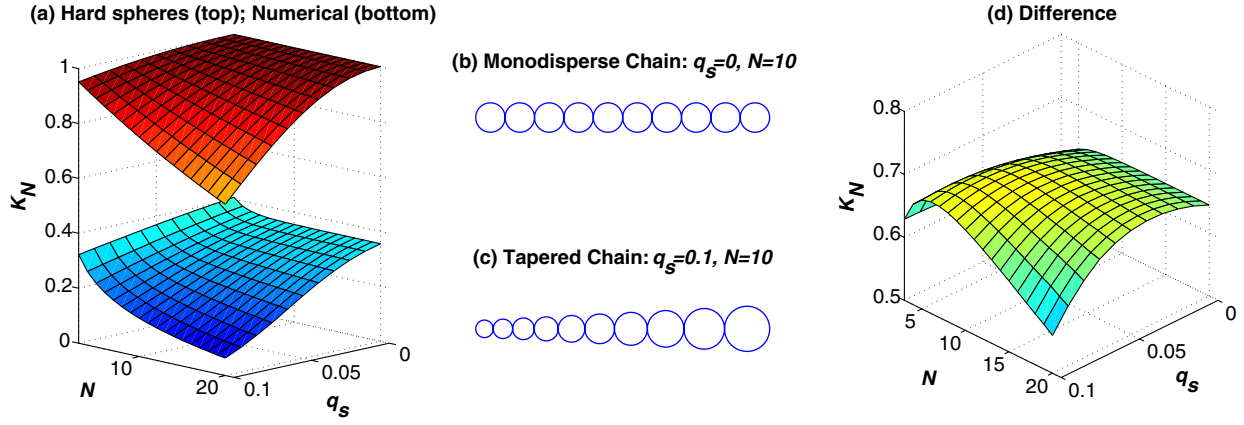

FIG. 1 (color online). (a) Hard-sphere approximation and numerically solved normalized kinetic energy surfaces, $K_N \equiv K_{\mathrm{OUT}}/K_{\mathrm{IN}}$, for the simple chain as functions of the number of spheres, N, and tapering, q_s. Their difference is plotted in panel (d) with a reduced z axis. Sample tapered chains are identified in panels (b) and (c).

numerical results presented here ignore energy losses, and since all real systems will have several modes of energy dissipation—friction, rolling, slipping, sound, etc.—this surface represents the worst case. In these numerical studies we use the velocity-Verlet [15] algorithm with a time step of 10 ps integrated over 10^8 steps. In addition, energy is conserved to about one part in 10^{12}.

The reason for the difference between the approximation and the numerical solution in Fig. 1(a) is, of course, due to the potential. For hard spheres, the sequence consists of independent collisions [16] where the velocity ratio is $v_{i+1}/v_i = 2/[1 + (1 - q_s)^3]$. Since the potential is infinite, energy and momentum are transferred instantaneously. Further, the hard spheres are not confined and momentum always carries them *forward* after interacting. Numerically, rebounding occurs. Even if $q_s = 0$—i.e., inertial matching—the natural partitioning of energy seen numerically is not accounted for by the approximation. Thus, for hard spheres, all of the energy is kinetic as compared to about 56.5% when the numerical-based analysis is performed. These differences are plotted directly in Fig. 1(d).

It is clear that the best energy absorption occurs for highly tapered chains where there are a large number of spheres. Unfortunately, large values of N may not be realizable for many applications where space is at a premium. The natural scalability may be used to drive the system to smaller sizes, but manufacturing issues may become restrictive. And while precompressing the chain can further increase the amount of absorption [17], that condition needs to be externally maintained throughout the dynamics. How does one then apply short tapered chains where substantial energy mitigation is needed?

Larger and more frequent inertial mismatches lead to better momentum traps and energy dispersion. We therefore propose an improved tapered chain design in which we place interstitial grains at the particle contacts of a simple chain. We refer to this as the decorated chain [examples shown in detail later in Figs. 3(d)–3(i)]. The latter is essentially a modified simple chain where we have introduced interstitial grains of constant radius, fr_N, between every member of the simple chain, where $0 < f \leq 1.0$ and r_N is the radius of its smallest bead. The relation, fr_N, was chosen for convenience in deriving a hard-sphere approximation. From this point on, q appears in both simple and decorated chains but is defined differently. As such, they are denoted as q_s and q_d, respectively. We constrain the decorated system to an odd number of particles such that the grains that formed the ends of the simple chain are still the outer members. A hard-sphere derivation for the decorated chain [18] is cumbersome and only key points are presented here. The conservation equations for mass and energy are carried out for several terms until a pattern emerges. The velocity ratio is given by

$$\frac{v_N'}{v_1} = (2A^{1/2})^{(N-1)} \prod_{j=1}^{(N-1)/2} \left(\frac{\epsilon^{3(j-1)}}{A + \epsilon^{3(j-1)}}\right)\left(\frac{1}{\epsilon^{3j} + A}\right), \quad (3)$$

where $A \equiv f^3\epsilon^{3(N-1)/2}$, $\epsilon \equiv (1 - q_d)$, and q_d is now defined as $R_{i+2}/R_i = (1 - q_d)$.

Turning to the mass ratios, we find that

$$\frac{m_N}{m_1} = \epsilon^{3(N-1)/2}. \quad (4)$$

We can now identify the normalized kinetic energy by squaring Eq. (3) and combining it with (4) to form

$$K_N = (4A\epsilon^{(3/2)})^{(N-1)} \left\{ \prod_{j=1}^{(N-1)/2} \frac{\epsilon^{3(j-1)}}{(A + \epsilon^{3(j-1)})(\epsilon^{3j} + A)} \right\}^2. \quad (5)$$

Figure 2 sketches this distribution.

It is difficult to draw any physical intuition from (5). However, a very curious and astonishing result occurs in the limit $q_d = 0$. Under that condition, (5) reduces to

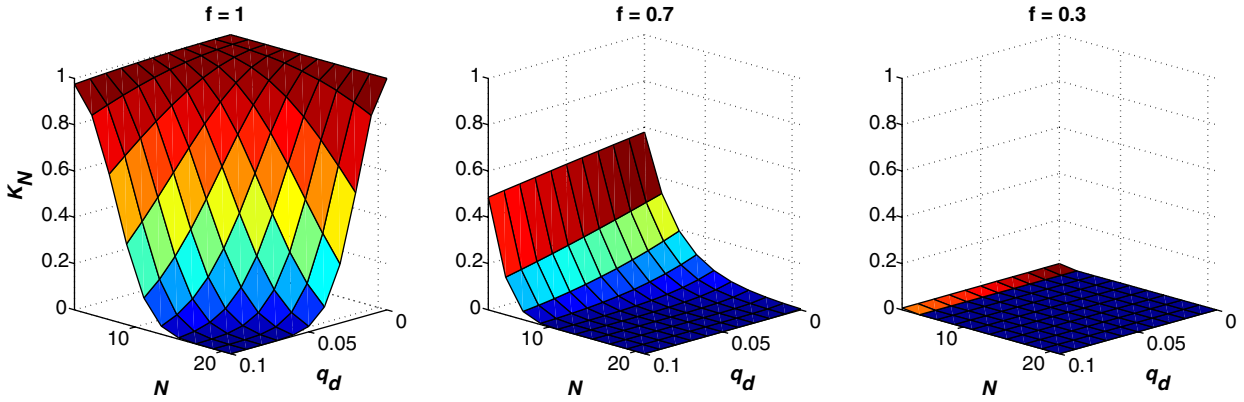

FIG. 2 (color online). Normalized kinetic energy surfaces, $K_N \equiv K_{\mathrm{OUT}}/K_{\mathrm{IN}}$, for the decorated chain under the hard-sphere approximation as functions of the number of spheres, N, fractional size of interstitial sphere, f, and tapering, q_d.

$$K_N|_{q_d=0} = \left(\frac{4f^3}{[f^3+1]^2}\right)^{N-1}. \tag{6}$$

This limit is equivalent to Eq. (1) under the exchange $f \Leftrightarrow (1 - q_s)$. As a result, K_N decays as a half-Gaussian or sigmoid with increasing f, and exponentially with increasing N. It is clear that $f = 1$ should imply $q_s = 0$ since they both generate monodisperse chains. That this equivalency goes beyond that special case is quite unexpected. One can now begin to see the incredible effect f has on the energy mitigation capability when an infinite potential is invoked: for $f = 0.3$—a typical value we might consider—the equivalent tapering in the simple chain would be $q_s = 0.7$. This value is 7 times larger than any system we had previously considered and could be a significant system integration challenge. Visually, for hard spheres, the energy mitigation capability of the simple chain shown in Fig. 1(c) ($q_s = 0.1$) is identical to that for a decorated chain similar to that shown in Fig. 3(d) but with $q_d = 0$, $N = 10$, $f = 0.9$.

Figure 3 highlights the computational results for the decorated chain. Figures 3(d)–3(i) demonstrate the wide variety of systems possible given f, q_d, and N. It is immediately clear that the inertial mismatch changes as a

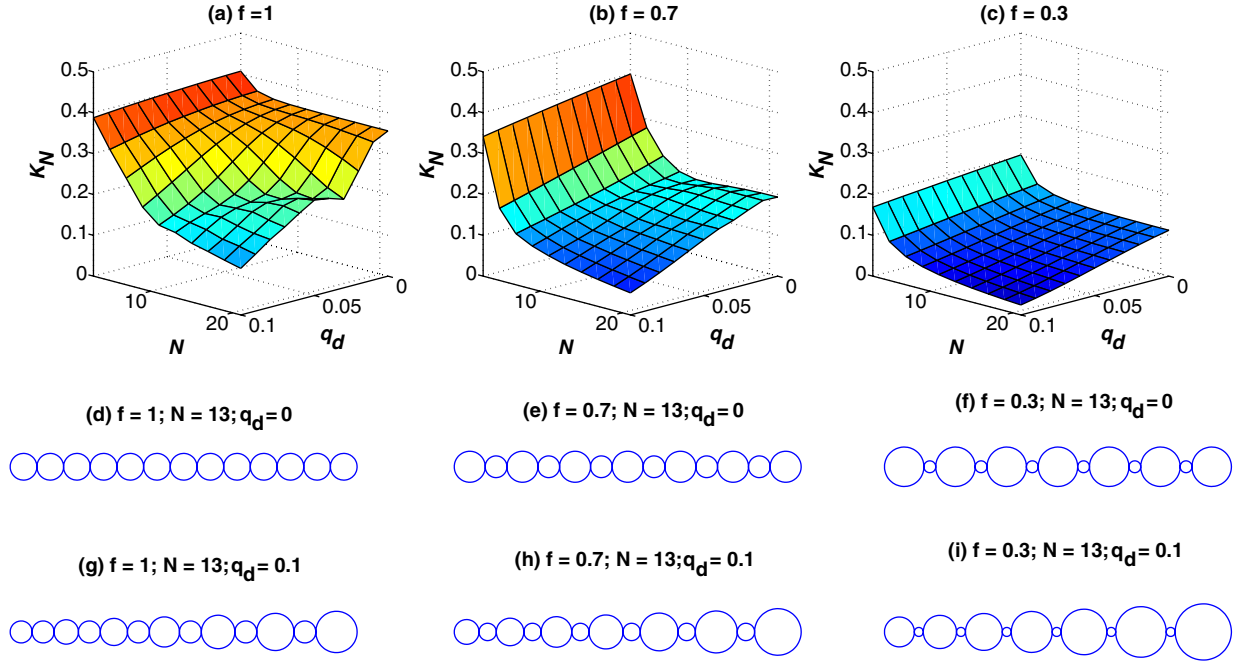

FIG. 3 (color online). (a)–(c) Numerically produced normalized kinetic energy surfaces, $K_N \equiv K_{\mathrm{OUT}}/K_{\mathrm{IN}}$, for the decorated chain as functions of the number of spheres, N, fractional size of interstitial sphere, f, and tapering, q_d. Several sample chains are identified in panels (d)–(i).

function of position along the decorated chain—a dynamic not present for the simple chain. It is possible then to have decorated chains that appear monodisperse ($q_d = 0$) for only a subset of the chain. This is what we believe to be the cause of a ripple in the surface of the K_N plots that propagate toward the origin as f decreases. As one might expect, such behavior would be functions of N, q_d, and f. The effect vanishes for $f \leq 0.6$, approximately. At about this threshold, the interstitial grain is not much smaller (less massive) than the grains toward the end of the chain. The explanation is that as an impulse propagates, energy transmission becomes increasingly efficient due to smaller inertial mismatches—a prerequisite for admitting solitary waves [19,20]. Thus the system changes from a shock absorber to a shock transmitter. This effect, however, must compete with compressive effects in some manner since no such behavior is present for hard spheres even though it too has a position-dependent inertial mismatch.

Simulations suggest that for $f = 0.3$, $N = 5$, $q_d = 0.1$, one can disperse energy within the chain such that only about 10% of that put into the system is transmitted to the end with the initial pulse. At later times, the pulse is converted into noise.

To conclude, granular alignments are rich, highly scalable, nonlinear dynamical systems that can be constructed to act as shock absorbing systems. They can be tuned by modifying the material properties and contact geometries, producing fascinating and sometimes unexpected outcomes. Both system types can be realized—and have been corroborated experimentally. In point, an experimental study by Agui [21] at NASA—Glenn Research Center on a decorated chain with $q_d = 0.05$, $f \sim 0.3$, $N = 9$ reveals that the force felt by the last grain is approximately 50% of that compared to a simple chain of similar length.

A hard-sphere approximation for the simple chain correctly describes the functionality of N and q_s for the normalized energy parameter space. The softness of the potential is a factor but not a dominant one. The decorated chain, much to our surprise however, cannot be described by such an approximation because shock transmission properties vary with position along the chain, and the softness of the spheres—due to the Hertz potential—strongly influence that behavior. This particular system, consequently, cannot be treated by an independent collision model. As a note of academic interest and in considering hard spheres, the limit of $q_d = 0$ for the decorated chain surprisingly reduces to that for the simple chain under the exchange, $f \Leftrightarrow (1 - q_s)$. This says that a hard-sphere chain consisting of an alternating series of radii (where $r_{\text{small}} = f r_{\text{large}}$) has the kinetic energy absorption equivalency of a simple chain of tapering q_s.

The authors would like to thank Dr. John Powell, Professor Dan Mattis, and Professor Jayanth Banavar for their review of and interest in this work. R. D. thanks the U.S. Army Research Laboratory for their continuing financial support of this work. S. S. acknowledges support from the U.S. Army Research Office. We thank Dr. Agui for his permission to include details of his study prior to publication.

*Electronic address: bdoney@arl.army.mil
†Electronic address: sen@dynamics.physics.buffalo.edu

[1] S. Sen, F. S. Manciu, and M. Manciu, Physica (Amsterdam) **299A**, 551 (2001).
[2] R. L. Doney and S. Sen, Phys. Rev. E **72**, 041304 (2005).
[3] S. Job, F. Melo, A. Sokolow, and S. Sen, Phys. Rev. Lett. **94**, 178002 (2005).
[4] M. Nakagawa, J. H. Agui, D. T. Wu, and D. V. Extramiana, Granular Matter **4**, 167 (2003).
[5] F. Melo, S. Job, F. Santibanez, and F. Tapia, Phys. Rev. E **73**, 041305 (2006).
[6] R. Frey, N. Gniazdowski, T. H. Li, and F. Tarzian, Army Research Laboratory Technical Report No. ARL-TR-3668, 2005.
[7] B. Gama, T. A. Bogetti, B. K. Fink, C. J. Yu, T. D. Claar, H. H. Eifert, and J. W. Gillespie, Composite Structures **52**, 381 (2001).
[8] A. M. Hayes, A. Wang, B. M. Dempsey, and D. L. McDowell, Mech. Mater. **36**, 691 (2004).
[9] R. Frey (private communication).
[10] H. A. Bruck, Int. J. Solids Struct. **37**, 6383 (2000).
[11] H. Hertz, J. Reine Angew. Math. **92**, 156 (1881).
[12] L. D. Landau and E. M. Lifshitz, *Theory of Elasticity* (Pergamon Press, Oxford, 1970), p. 30.
[13] A. Sokolow (private communication).
[14] R. L. Doney (unpublished).
[15] M. P. Allen and D. J. Tildesley, *Computer Simulation of Liquids* (Clarendon, Oxford, 1987).
[16] D. Wu, Physica (Amsterdam) **315A**, 194 (2002).
[17] A. Sokolow, J. M. M. Pfannes, R. L. Doney, M. Nakagawa, J. H. Agui, and S. Sen, Appl. Phys. Lett. **87**, 254104 (2005).
[18] R. L. Doney and S. Sen, Army Research Laboratory Technical Report No. ARL-TR-3612, 2005.
[19] V. F. Nesterenko, J. Appl. Mech. Tech. Phys. **5**, 733 (1983).
[20] S. Sen and M. Manciu, Phys. Rev. E **64**, 056605 (2001).
[21] J. H. Agui, Jr. (to be published).